Electronic Supplementary Material (ESI) for Nanoscale.

-Supporting Information-

Design and Characterization of Plasmonic Doppler Grating for Azimuthal Angle-resolved Surface Plasmon Resonances

Kel-Meng See,[1,†] *Fan-Cheng Lin* [1,†] *and Jer-Shing Huang*[1,2,*]

[1] Department of Chemistry, National Tsing Hua University, Hsinchu 30013, Taiwan

[2] Leibniz Institute of Photonic Technology, 07745 Jena, Germany

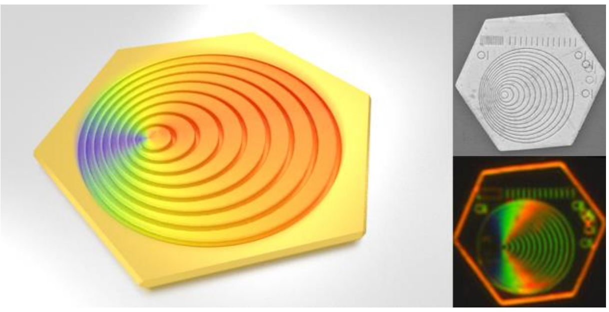

*Correspondence should be addressed:

jer-shing.huang@leibniz-ipht.de

[†]These authors contribute equally to this work.

I. Derivation of PDG periodicity

The trajectory of PDG can be mathematically expressed as

$$(x - nd)^2 + y^2 = (n\,\Delta r)^2,\ d < \Delta r,\ ,\ n \geq 1 \qquad \text{(SI-1)}$$

, where Δr is the radius increment , d is the center displacement of circular ring relative to the adjacent rings and n is the sequence number of the rings. To derive the periodicity P as a function of φ, we first write the trajectory of PDG into polar coordinate as

$$(R_n \cos\varphi - nd)^2 + (R_n \sin\varphi)^2 = (n\,\Delta r)^2,\ d < \Delta r \qquad \text{(SI-2)}$$

, where R_n is the radius and φ is the azimuthal angle. Specifically, R_n represents the distance between the origin and the point on n^{th} ring and can be solved from relation above as

$$R_n = nd\cos\varphi \pm \sqrt{n^2(d^2\, cos\, 2\varphi + 2\Delta r^2 - d^2)/2}\ ,\ d < \Delta r \qquad \text{(SI-3)}$$

In polar coordinate, two real solutions of R_n can be mathematically solved for each chosen φ, with one positive value and one negative value. The positive and negative solutions correspond to the solutions along azimuthal angle φ and $\varphi + 180°$ in the Cartesian coordinate, respectively. Following the above results, the grating periodicity $P_{\Delta r,d}(\varphi)$ can be obtained by calculating $|R_{n+1} - R_n|$. The calculation leads to an azimuthal angle-dependent function as

$$P_{\Delta r,d}(\varphi) = \left|dcos\,\varphi \pm \sqrt{(d^2\, cos\, 2\varphi + 2\Delta r^2 - d^2)/2}\right|,\ d < \Delta r \qquad \text{(SI-4)}$$

An absolute sign is added to the solutions in order to return the periodicity into a scalar. Similarly, two solutions of periodicity can be obtained for each chosen φ. The solutions correspond to periodicities along azimuthal angles φ and $\varphi + 180°$ of PDG. Since n is cancelled by $|R_{n+1} - R_n|$, PDG provides periodic grating with periodicity depends only on r, d and φ but not n. By carefully choosing Δr and d, the periodicity on PDG can be designed to vary from maxima $\Delta r + d$ to minima $\Delta r - d$ as the azimuthal angle is scanned from $0°$ to $180°$. This makes PDG a flexible platform that can be easily designed for best performance.

II. Optical Setups

In the dark-field scattering experiment, white-light illumination (HAL 100 illuminator with quartz collector, Zeiss) is impinging the sample from the ITO substrate with Köhler illumination scheme using an oil condenser (Achromatic-aplanatic Condenser N.A. = 1.4, Zeiss). The scattered light is then collected by another objective (MPlanApo 60X air N.A. = 0.9, Olympus) on the side open to air and is aligned either onto a color CCD (PMD-130, OME-TOP SYSTEMS CO., LTD.) to obtain color images or onto a spectrometer to record the azimuthal angle-resolved spectra. To record the spectra, two linear polarizers (LPVIS100-MP, 550-1500 nm, Thorlabs) are inserted into the excitation and detection optical pathways to select the azimuthal angles. Bandpass filters with finite bandwidth of 40 nm (FKB-VIS-40, Thorlabs) are used to obtain narrow band excitation centered at 550 nm, 600 nm, 650 nm and 750 nm. The optical characterization of PDG color sorter is performed both in reflection mode and in transmission mode. In the reflection mode, unpolarized white light source is used to illuminate the PDG with a nearly normal incident angle. The incident light and the reflected light are collected using the same air objective (DIN PLL 20 X, N.A. = 0.4, ZAK). For the transmission mode, the incident light is softly focused onto the sample with a microscope condenser (Air, N.A. = 0.3, Zeiss) and the transmitted light is collected by an oil objective (Plan-Apochromat 63X oil Iris, N.A. = 0.7-1.42, Zeiss). Schematic diagrams for the optical setups used in the scattering mode, reflection mode and transmission mode are shown in Figs. S3(A), S3(B) and S3(C), respectively.

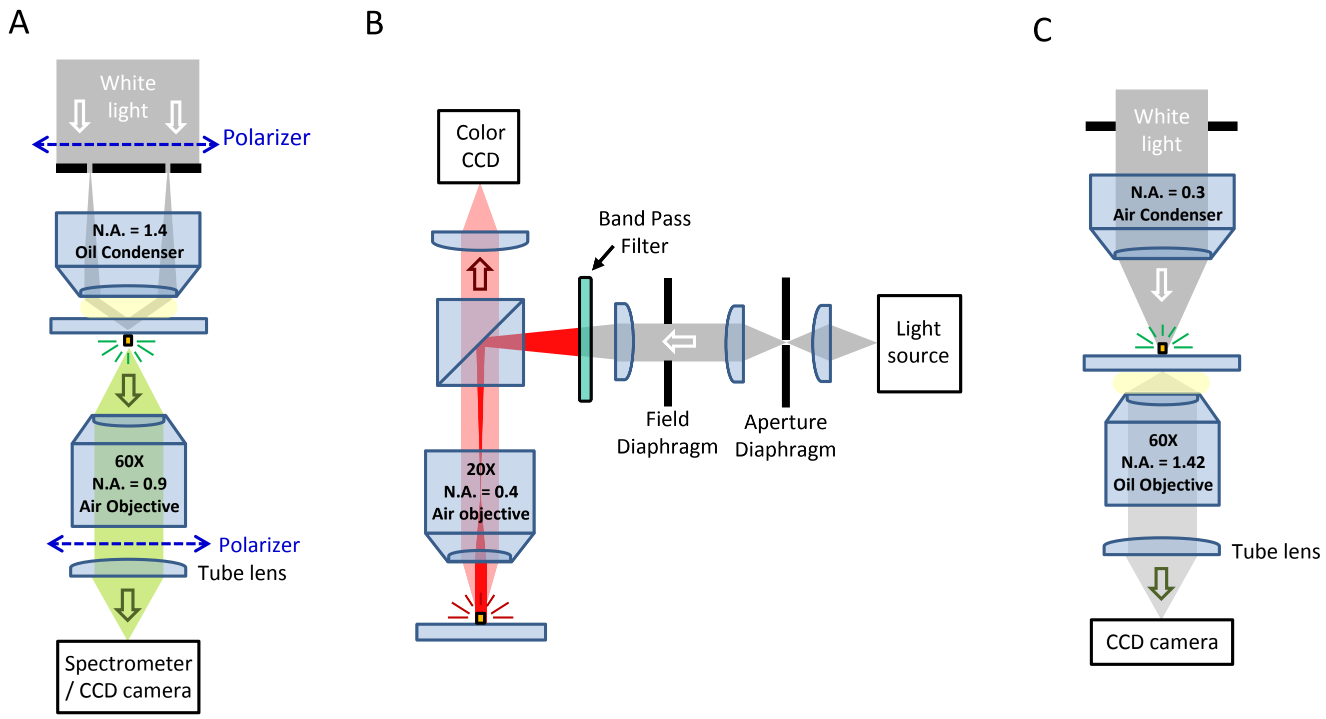

Figure S1. Setups used for optical characterization. (A) Scattering microscope setup using oil condenser with high numerical aperture for obtaining dark-field scattering spectra and images. (B) Reflection microscope using near-normal white light illumination for obtaining reflection spectra and images. (C) Transmission microscope setup for obtaining transmission spectra and images.

III. Collection Limitation

Equation **1** in the main text describes the coupling between photons and surface plasmons (SPs). According to reciprocity, the incident angle of photons, α, in equation (1) also represents the out-coupling angle of SPs to the far field. To detect such signals experimentally, the out-coupling angle of SPs must be within the collection angle of the microscope objective. Light scattered by the PDG with an angle beyond the collection range of the objective will not be seen in the experimental spectra. Such limited collection angle of the microscope objective is the major reason for the missing spectral features in the experimental spectra compared to the simulated ones. The spectral region that is undetectable in our system can be analytically solved for the numerical apertures of the objectives. The blue shaded region in Fig. S2 marks the spectral region, where out-coupling angle α is larger than the objective collection angle, 60°. For SP resonance with m = -1 at Au/ITO interface, the experimental spectra shows a cut-off within the window of azimuthal angle between 60° to 90°. This explains why the resonance mode of m = -1 at Au/ITO only appears in the simulations (see right panel in Fig. 2d). As shown on the right panel of Fig. S2, most of the scattering light from the grating area with small periodicity (marked with dotted-lined area in the inset of Fig. S2) is out of the collection angle of the objective. This is why this region appears to be dark in the images (right panel of Fig. 2b) and the corresponding SP resonant peaks are all missing in the experimental spectra compared to the simulated ones (Fig. 2d).

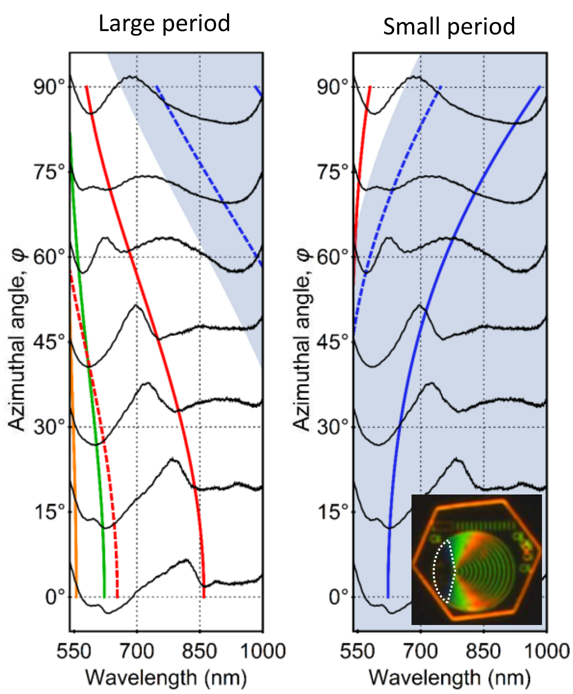

Figure S2. The resonance modes for grating of large period (left panel) and small period (right panel) along each azimuthal angle are plotted separately with the azimuthal angle-resolved scattering spectra obtained from the dark-field scattering experiment. The shaded parts mark the undetectable area calculated from analytical model with parameters of $\alpha > 60°$, $m = -1$, $d = 200$ nm, $\Delta r = 400$ nm, $n_d = 1$ and $n_i = 1$ using ε_m for gold.

IV. Image Analysis and Fitting

To quantify the angle distribution of the intensity, we have analyzed the reflection and transmission images taken under the narrow band excitation at 550 nm, 600 nm and 650 nm and plot the intensity as a function of azimuthal angle. The color images recorded by CCD is an M×N×3 matrix that represents the red (R), green (G) and blue (B) components of M×N pixels. These images are first spatially filtered by a mask to remove the pixels out of the relevant region of the PDG. For transmission images, the mask is applied such that only the signal from the region of the circular air slit ring is analyzed. The spatially filtered color images are then converted into grayscale intensity image using the standard default RGB color space, *i.e.* $\mathrm{I} = 0.2989\mathrm{R} + 0.5870\mathrm{G} + 0.1140\mathrm{B}$. The obtained intensity profiles are then normalized to the maximum intensity. The azimuthal angle for each pixel is determined by using the following equation,

$$\varphi[i,j] = \tan^{-1}\frac{-i+i_0}{j-j_0} \qquad \text{(S1)}$$

, where *i* and *j* are the pixel coordinates at the *i*-th row and *j*-th column of the matrix, while i_0 and j_0 are the pixel coordinate at the origin of the PDG, *i.e.* the position of the smallest ring with zero diameter. The normalized intensity is then plotted as a function of the azimuthal angle to yield the intensity angle distribution profile. To quantitatively determine the azimuthal angle of the resonance band, intensity angle distribution profiles are fitted with the following function,

$$I(\varphi) = \sum_m \left(\frac{\left(\frac{P(\varphi+x_0)^2 - P(\varphi_m)^2}{2\,w_m P_m} + q_m\right)^2 + b_m}{\left(\frac{P(\varphi+x_0)^2 - P(\varphi_m)^2}{2\,w_m P_m}\right)^2 + 1} - 1 \right) \cdot \sqrt{(\cos(\varphi + x_0 - \gamma))^2 + (1-\eta)(\sin(\varphi + x_0 - \gamma))^2} \cdot A_m + y_0 \qquad \text{(S2)}$$

$I(\varphi)$: reflection intensity at azimuthal angle φ
m: resonance order
$P(\varphi)$: azimuthal angle-dependent periodicity described by Eq. (2)
$P(\varphi_m)$: resonant grating periodicity for the m^{th}-order resonance
w_m: spectral width of the Fano resonance for the m^{th}-order resonance
q_m: asymmetry parameter for the m^{th}-order resonance
b_m: modulation damping parameter for the m^{th}-order resonance
γ: angle between incident light polarization and the edge of the rings
η: degree of polarization of the excitation in the experiment
A_m: amplitude of the m^{th}-order resonance
y_0: amplitude offset
x_0 : angle offset

With the fitting, the grating periodicity for the m^{th} order SP resonance, $P(\varphi_m)$, can be determined. Consequently, by applying the fitted value of the periodicity to Eq. 2, we can obtain the azimuthal angle of the SP resonance. The fitting function shown in Eq. S2 is based on a Fano-like resonance model[38] and takes into account the broadening due to the loss of SPs, the coupling to dark modes, the degree of polarization of the illumination and the incident polarization angle with respect to the PDG grating edge. The parameters for fitting the experimental data in Fig. 3 are summarized in Tables S1 and S2.

Table S1. Parameters for fittings in Fig. 3c (reflection) in the main text (Bandpass filter centered at 550 nm, 600 nm and 650 nm)

Parameters		Wavelength		
		550 nm	600 nm	650 nm
P_m (nm)	$m = -1$	323.40	444.78	495.37
	$m = +1$	533.21	557.06	604.59
w_m (nm)	$m = -1$	183.51	75.90	69.52
	$m = +1$	20.21	12.78	14.02
A_m	$m = -1$	0.92	0.82	0.81
	$m = +1$	0.22	0.05	0.06
q_m	$m = -1$	-0.15	-0.06	-0.058
	$m = +1$	-0.18	-1	-1.14
b_m	$m = -1$	0.14	0.21	0.24
	$m = +1$	0.01	0	0
Δr (nm)		400		
d (nm)		200		
κ		0.20	0.20	0.2
γ (^{0})		94.39	94.39	94.39
y_0		1.02	0.83	0.84
x_0		0		

Open angle 2φ & Coefficient of determination R^2

2φ(^{0})	$m = -1$	193.68	128.1	101.48
	$m = +1$	79.22	62.72	
R^2		0.82	0.81	0.80

Table S2. Parameters for fittings in Fig. 3d (transmission) in the main text (Bandpass filter centered at 550 nm, 600 nm and 650 nm)

Parameters		Wavelength		
		550 nm	600 nm	650 nm
P_m (nm)	$m = -1$	457.56	489.76	537.14
	$m = +1$	574.16	583.95	593.95
w_m (nm)	$m = -1$	53.86	60.73	44.42
	$m = +1$	7.30	14.62	9.15
A_m	$m = -1$	-0.63	-1.07	-0.94
	$m = +1$	-0.043	-0.22	-0.09
q_m	$m = -1$	0.64	0.24	0.21
	$m = +1$	0.63	-0.21	-0.92
b_m	$m = -1$	0.28	0	0.03
	$m = +1$	2	0	0
Δr (nm)		400		
d (nm)		200		
κ		0.28	0	0.04
γ (^{0})		101.05	0	48.07
y_0		-0.32	-0.07	-0.08
x_0		0		

Open angle 2φ & Coefficient of determination R^2

2φ(^{0})	$m = -1$	121.54	104.54	76.68
	$m = +1$	48.18	37.78	23.08
R^2		0.90	0.89	0.90